

## Atmospheric boundary layer observations on the East Coast at Kalpakkam using Doppler mini-sodar during different seasons

A. BAGAVATH SINGH, R. VENKATESAN, C. V. SRINIVAS\* and K. M. SOMAYAJI

*Radiological Safety Division, Indira Gandhi Centre for Atomic Research, Kalpakkam, India*

\*e mail : cvsri@igcar.ernet.in

**सार** – इस शोध पत्र में भारत के पूर्वी तट पर किए गए तटीय वायुमंडलीय परिसीमा स्तर प्रयोग (केबल) के दौरान आप्तिक स्थल कलपाकम के निकट अनुपुरम् में चरणबद्ध रूप से व्यवस्थित डॉपलर मिनि सोडार स्थापित किया गया। प्रदूषकों के तटीय प्रसरण का अध्ययन करने के लिए पवन प्रोफाइल को मापने हेतु और स्थल - समुद्र समीर परिसंचरण के कारण तटीय परिसीमा स्तर में हुई वृद्धि की जाँच करने के लिए मिनि सोडार का उपयोग किया गया। दक्षिणी पश्चिमी मानसून (13,14 अगस्त : आरमेक्स – I और 3, 7, 11, 14 सितंबर) तथा मानसून ऋतु से पूर्व की अवधि (27, 28 अप्रैल : आरमेक्स – II) 2003 के दौरान वायुमंडलीय परिसीमा स्तर की परिवर्तनशीलता का अध्ययन किया गया है। समुद्र समीर के चलने के दौरान बृहत् पवन दिशा में परिवर्तन और उच्च उर्ध्वधर वेग में परिवर्तनशीलताएं ज्ञात की गई हैं। तापीय आंतरिक परिसीमा स्तर (टी. आई. बी. एल.) की ऊँचाई में ऋतु के अनुसार उत्तरोत्तर वृद्धि होती है ; ग्रीष्म ऋतु – 170 मी., दक्षिणी पश्चिमी मानसून – 210 मी. और उत्तरी पूर्वी मानसून – 325 मी., जबकि नॉक्टयूरनल परिसीमा स्तर की ऊँचाई में तत्संबंधी अवधि में उत्तरोत्तर रूप में कमी आ जाती है ग्रीष्म ऋतु – 370 मी., दक्षिणी पश्चिमी मानसून – 340 मी. और उत्तरी पूर्वी मानसून – 210 मी.।

**ABSTRACT.** A phased array Doppler Mini-Sodar has been installed at Anupuram near Kalpakkam nuclear site during the Coastal Atmospheric Boundary Layer Experiments (CABLE) carried out on the east coast of India. Mini-Sodar was used to measure the wind profile and investigate the coastal boundary layer development due to land-sea breeze circulation for the study of coastal dispersion of pollutants. The atmospheric boundary layer, its variability during SW (August 13, 14 : ARMEX I and September 3, 7, 11, 14) and pre-monsoon period (April 27, 28 : ARMEX II) 2003 has been studied. Large wind direction change and high vertical velocity variance were observed during the onset of sea breeze. The Thermal Internal Boundary Layer (TIBL) height has been found to increase progressively with season: summer - 170 m, SW monsoon - 210 m and NE monsoon - 325 m whereas the Nocturnal Boundary Layer (NBL) height decrease progressively during the corresponding period: summer - 370 m, SW monsoon - 340 m and NE monsoon - 210 m.

**Key words** – ARMEX, Mini-sodar, Sea breeze, Thermal internal boundary layer, Nocturnal boundary layer, Turbulent kinetic energy, Tethersonde.

### 1. Introduction

The Atmospheric Boundary Layer (ABL) processes are very important for understanding the large scale atmospheric dynamics and for a large number of meteorological applications. The coastal boundary layer is heterogeneous due to variation in topography, land-sea thermal contrast and changes in surface roughness. Land-sea temperature gradient leading to the development of Thermal Internal Boundary Layer (TIBL) is a common feature in coastal sites (Garratt,1990). The air-sea exchange process is very much influenced by the terrain geometry in the coastal atmospheric boundary layer.

Acoustic remote sensing system - Sodar is now widely being used to measure the coastal boundary layer wind flow and turbulence pattern (Lenchow, 1986,

Somayaji, 1991, Thara Prabha *et al.* 1999, 2002). Mini-Sodar gives profiles of all three components ( $u$ ,  $v$ ,  $w$ ) of wind velocity from 15 - 460 m level with a vertical resolution of 10 m. The merit of the sodar is its ability to visualize the turbulence pattern of the atmospheric boundary layer structure and its variability. A portable Doppler phased array monostatic type Mini-Sodar has been installed (Bagavathsingh *et al.*, 2003) at Anupuram (Fig. 1) 5 km inland from Kalpakkam (12° 30' N, 80° 10' E) coastal site, as a part of the field experimental campaign to study the coastal atmospheric boundary layer. The vertical profiles collected using Mini-Sodar is used to study the coastal boundary layer during the ARMEX experiment.

The Mini-Sodar data collected during SW (July-September 2002 : ARMEX-I), and in pre-monsoon period

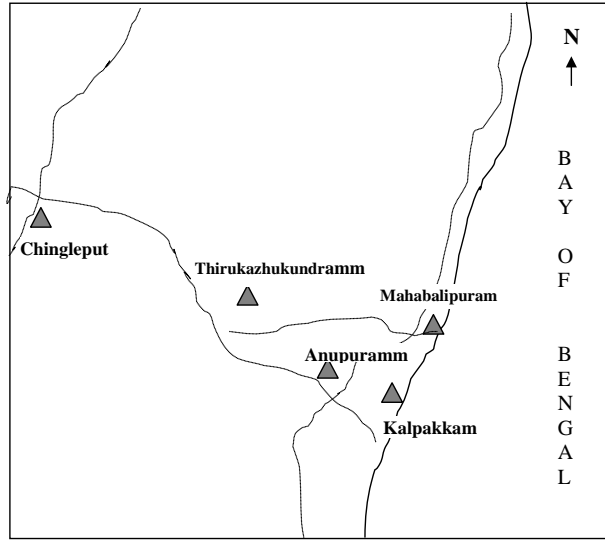


Fig. 1. Experimental site at Anupuramm (not to scale)

of (April - May 2003 : ARMEX-II) are analyzed. The measurements on wind components (horizontal and vertical), wind direction, their standard deviation, turbulence kinetic energy and its variability on different days are presented. These parameters are mainly gathered to characterize the vertical diffusion and transport processes for atmospheric dispersion and to understand the coastal boundary layer development during different phases of Indian monsoon.

## 2. Description of phased array type Mini-Sodar

The Scintec make phased array sodars are monostatic type (Scintec, 2001), that generate different beam angles during emission by phase delayed driving and sensing respectively of the rows and columns of an array of 64 acoustic transducers in a flat array configuration. It has an active antenna, an audio power driver for emission and audio preamplifier for reception mode. For transmission/reception highly efficient transducers are used. The time delay in transmission and reception modes is produced digitally. The system sends acoustic pulses in a cycle in 5/9 beam directions *i.e.*, 5 in V/N/E/S/W directions with a beam angle  $19^\circ$  and 4 in mirrored directions in N/E/S/W with a beam angle  $22^\circ$ . The system is configured such that each beam direction consists of 10 pulses in a sequence. Pulses are always between main and mirrored one. For the present study the system was operated in single frequency (3823 Hz) mode with data averaging time of 20 minutes.

In order to minimize/reduce stray noise emitted and reduce instrument susceptibility to active and passive

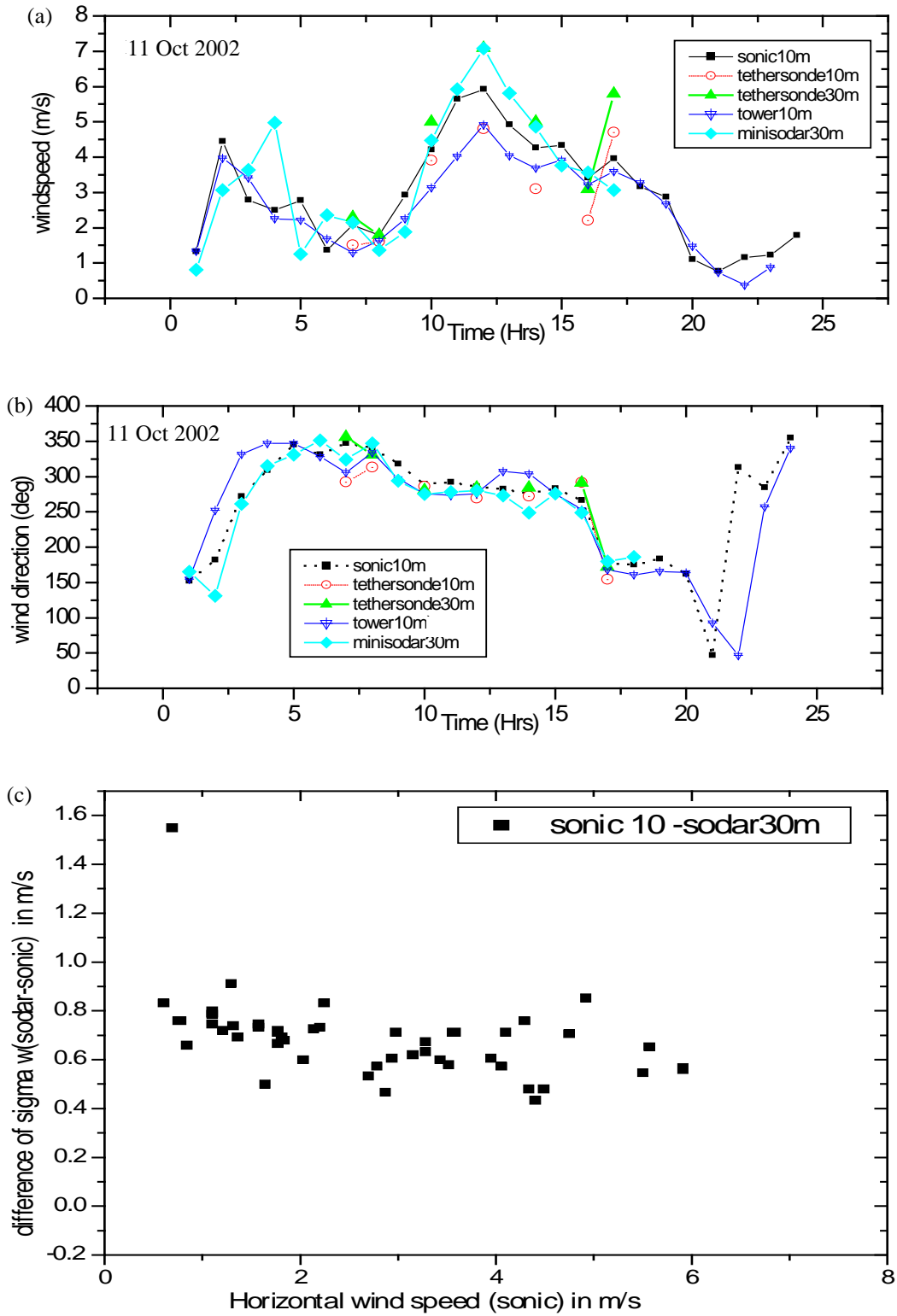


Fig. 2. Mini-Sodar antenna and enclosure

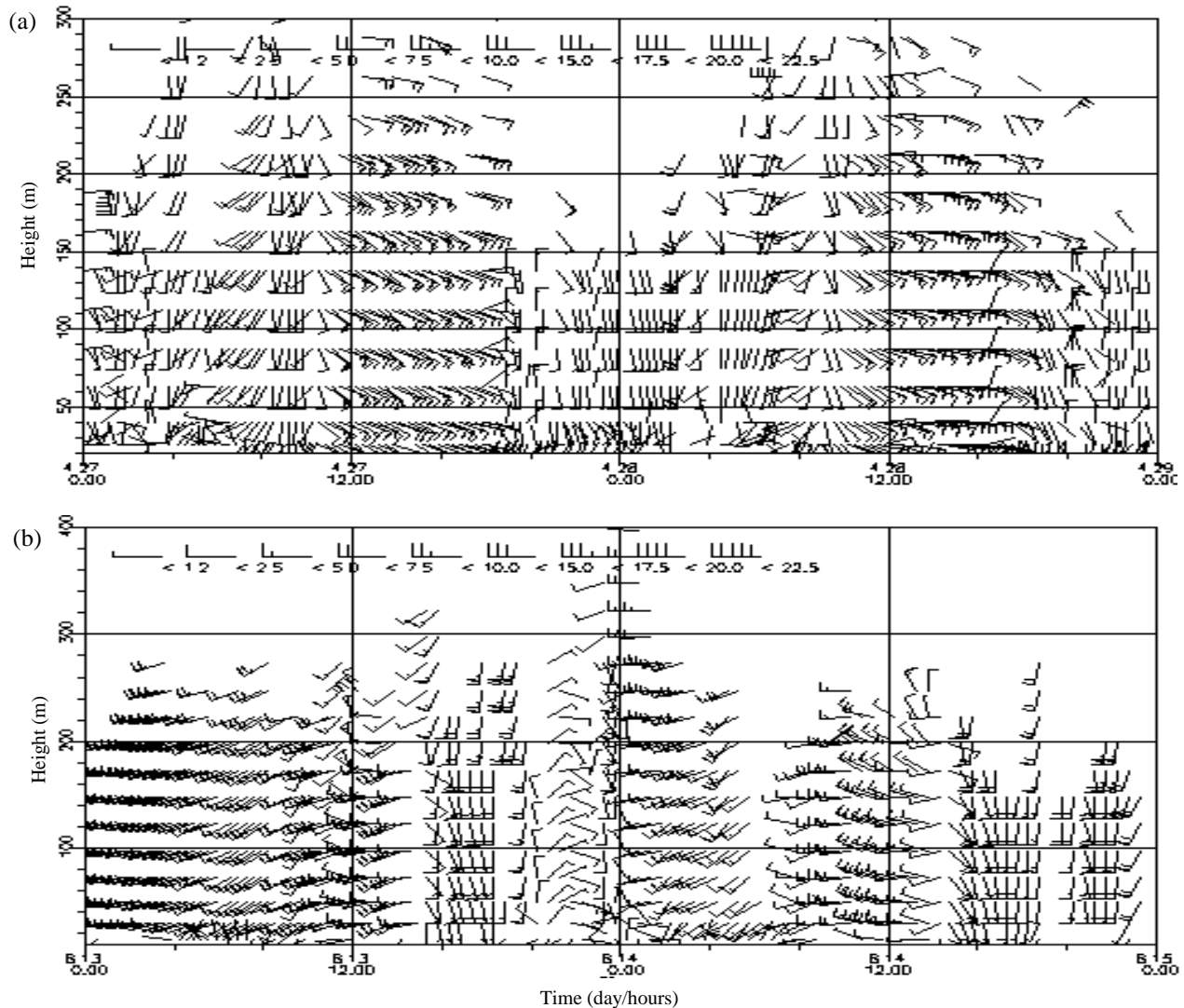
noise (including fixed echoes), an acoustic enclosure was mounted to the acoustic antenna. Fig. 2 shows the phased array antenna with the enclosure. The technical specifications of SFAS64 sodar are shown in Table 1.

### 2.1. Mini-Sodar performance

To evaluate the performance and reliability of the data, an objective comparison was made with near by 50 m tower- based *in situ* instruments. Comparison has also been made against measurements obtained by tethered flights and sonic anemometer. The sodar was initially placed at a distance of  $\sim 25$  m from tower. Fixed echoes from the 50 m meteorological tower were noticed and the sodar was moved to a suitable location 400 m away. As the terrain is nearly even, the data from different instruments could be compared. Figs. 3 (a&b) shows a comparison of wind speed and direction measured by sodar with different sensors. The wind direction shows close agreement among various measurements. Wind speed from Mini-Sodar at 30 m has been compared with tower data at 10 m level. As expected from the surface layer wind profile laws, Mini-Sodar data at 30 m height has shown an increase of wind compared to that at 10 m AGL on the tower. Sodar derived wind speed is higher than that of the tower data by about  $0.6-1.0 \text{ ms}^{-1}$ . Wind direction measured by sodar agrees well with the tower. The sodar derived  $\sigma_w$  is known to have systematic errors due to volume averaging (Crescenti, 1997). Sodar overestimates  $\sigma_w$  by about  $0.5-0.9 \text{ ms}^{-1}$ . The difference between  $\sigma_w$  values from Mini-Sodar and sonic anemometer is shown in Fig. 3(c).



**Figs. 3(a-c).** Comparison of (a) wind speed and (b) direction between sonic anemometer, cup anemometer and tethersonde at 10 m AGL and tethersonde and minisodar at 30 m AGL and (c) Difference of  $\sigma_w$  measured by sodar and sonic anemometer as a function of wind speed as measured by sonic anemometer



**Figs. 4(a&b).** Wind flow profile measured by sodar during different seasons (a) Pre monsoon 2003 and (b) SW Monsoon 2002

### 3. Data analysis

#### 3.1. Observed wind pattern

With the onset of SW monsoon the large scale flow becomes south-westerly but near the coast within the ABL there is meso-scale circulation of land – sea breeze induced by the temperature contrast between land and ocean. The sea breeze circulation is opposite to the monsoon flow on the east coast. Internal (thermal) boundary layer develops over the land due to step change in surface roughness and temperature across the coast. The wind vector plot of Sodar for the case of summer months

(27- 28 April, 2003) in Fig. 4(a) shows an early onset of sea breeze around 1030-1230 hr (IST). Abrupt changes in wind direction and turbulence are noticed during the onset of sea breeze. The duration of sea breeze hours is more in summer months than during monsoon seasons [Fig. 4(b)]. Sea breeze occurs with SE, S winds about 65 -75% of time between noon to late evening hours (1200-2000 hr IST) in summer months. The average wind speed during sea breeze was of the order of 6-8  $\text{ms}^{-1}$  at a height of 150 m. The synoptic wind is weak during summer, which is conducive for occurrence of mesoscale land-sea breeze flows. The sea-land temperature difference is also enhanced in summer season. The sea breeze sets in early morning hours during summer and before the onset of sea

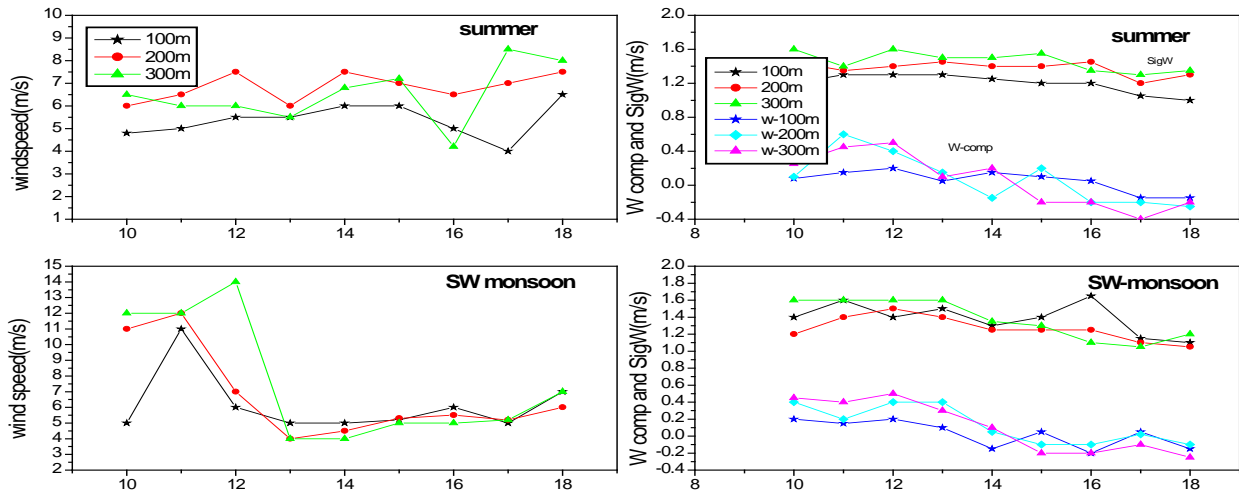


Fig. 5. Profiles of mean wind speed vertical wind ( $w$ ) component and  $\sigma_w$  during day in different seasons

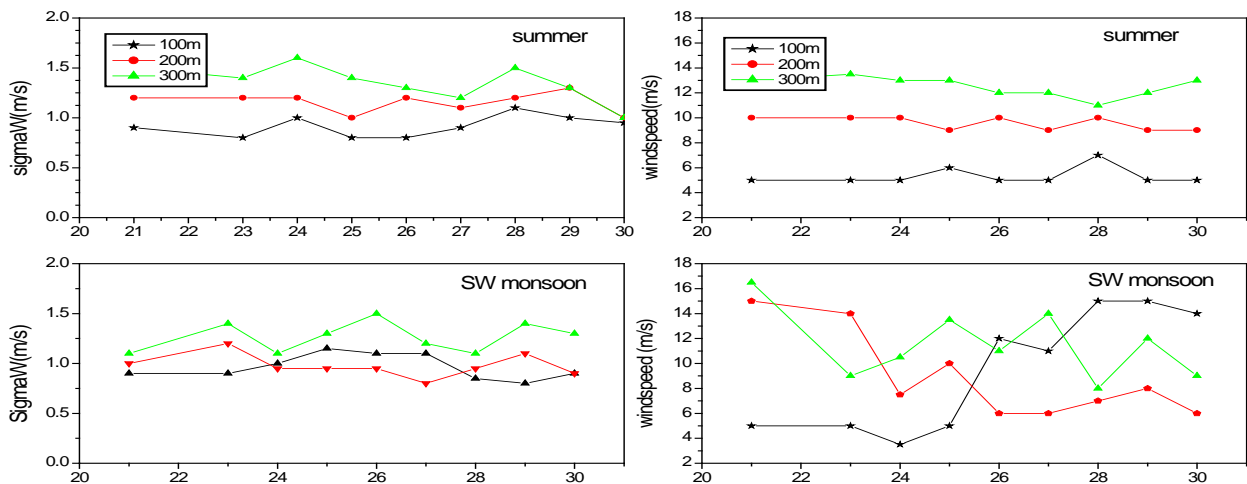


Fig. 6. Profiles of mean wind speed vertical wind ( $w$ ) component and  $\sigma_w$  night time in different seasons

breeze the sodar mean winds are observed to increase with height. After the onset of sea breeze there is a sea breeze inflow layer with a return current on top of it. Generally the sea breeze inflow layer extends upto 300-500 m (this is the max. range of Mini-Sodar measurements). There exists a shear in wind due to these two different currents (*i.e.*, sea breeze upto 300 m and winds opposite above it). As a result the strength of sea breeze decreases with height (Fig. 5) the 300 m wind speed is less than that at 100, 200 m height. This is not only observed during the summer but also in all seasons with some difference. In the SW monsoon season the onset of sea breeze occurs

late afternoon hours (1400-1630 hr IST) as shown in Fig. 4(b). In this season a maximum onshore wind of  $5-6 \text{ ms}^{-1}$  was observed during sea breeze below 200 m whereas above, a strong synoptic SW wind was observed.

Fig. 5 shows day time (1000-1800 hr IST) mean wind at 100, 200 and 300 m level. Data during night hour are shown in Fig. 6. During the SW monsoon the wind speed is high at 300 m level. Mini-Sodar performance during certain days, when echoes are weak, is poor at higher altitudes due to backscattered signal satisfying SNR (Signal to Noise Ratio) criteria are very few.

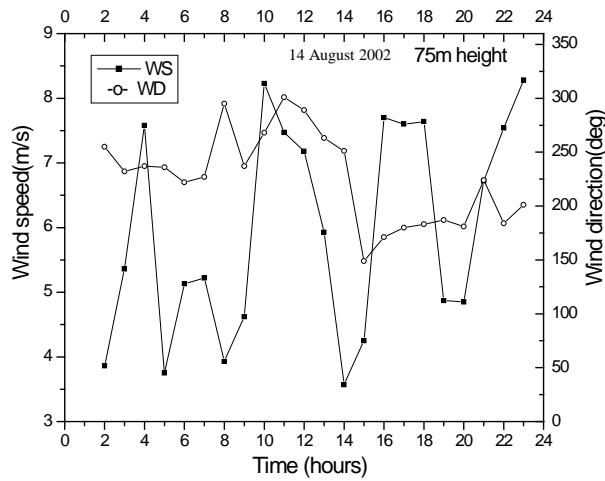
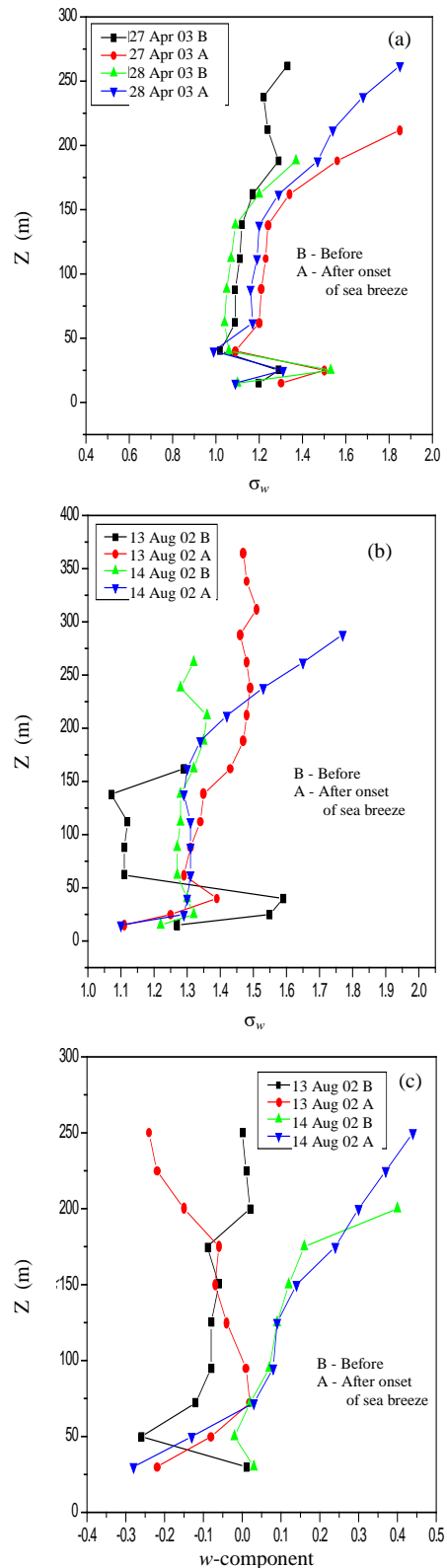


Fig. 7. Time series of wind speed and direction at 75 m AGL measured by sodar on 14 August 2002

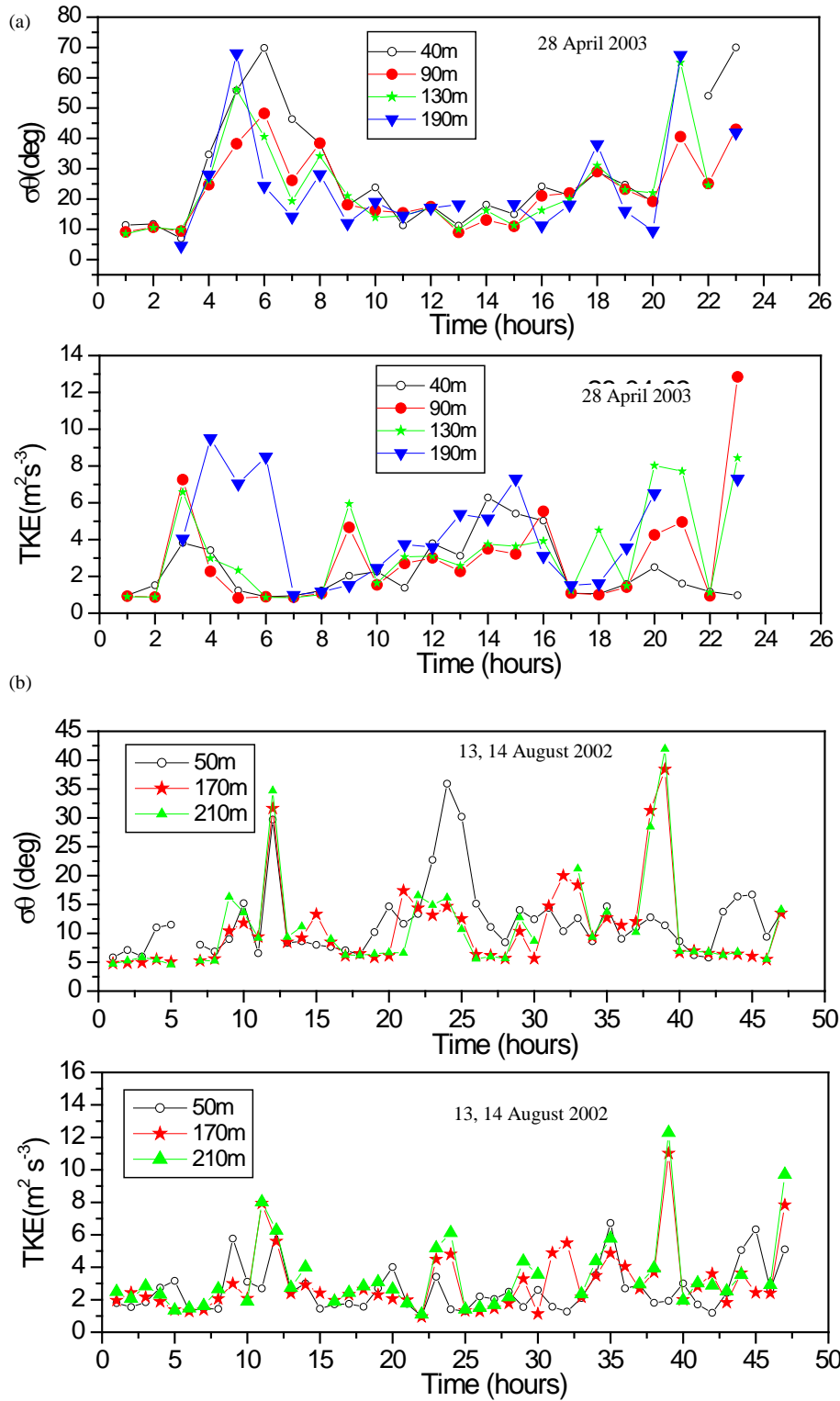
Averaging these small counts of data often leads to low wind speed estimates. During SW monsoon, the wind speed at 100-300 m level increases with height and is of the order of 10-14 ms<sup>-1</sup> around 1100 hr (IST), before the sea breeze onset. Fig. 7 shows the wind speed on 14 August 2002 during onset of sea breeze (1400 hr IST) when a dip in the wind speed just before sea breeze onset is observed clearly [Fig. 4(b)].

### 3.2. Turbulence pattern

The horizontal ( $\sigma_u, \sigma_v$ ) and vertical ( $\sigma_w$ ) turbulence intensity components are important for atmospheric stability characterization. Profile of  $\sigma_w$  observed before and after sea breeze onset is shown in Fig. 8(a) for a case in pre-monsoon (27, 28 April 2003) and Fig. 8(b) for SW monsoon (13, 14 August 2002) season. An increase in  $\sigma_w$  with height is observed at 30 m AGL in both cases. It is constant in the 50-150 m layer above during summer but the effect of sea breeze has shown an increase in turbulence beyond 150 m AGL. Similarly constant  $\sigma_w$  is observed between 50-100 m AGL before the onset of sea breeze on 13 August 2002. Fig. 8(c) shows the vertical wind component on 13-14 August 2002. The  $w$ -component is negative showing downdraft on 13 August whose vertical velocity was decreasing in the layer 25-75 m AGL and increasing above 75 m AGL after the onset. Before onset the downdraft vertical velocity was decreasing in the layer 50-250 m AGL. On 14 August the vertical velocity shows updraft in the layer before and after the onset of sea breeze. More case studies are required to interpret this data as it involves complex interactions of surface features with air circulation of



Figs. 8(a-c). Variation of  $\sigma_w$  with height before and after the onset of sea breeze in (a) Pre-monsoon 2003, (b) SW Monsoon 2002 and (c) for  $w$ -component



**Figs. 9(a&b).** Time series of profile of  $\sigma_\theta$  and turbulent kinetic energy (TKE) during different seasons

different scales. Numerical simulation of a sea breeze front may be necessary to model the complex interactions

of surface features with different scales of wind circulation.

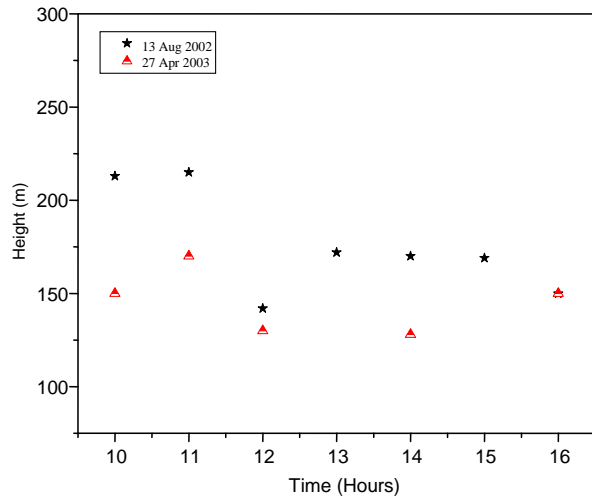


Fig. 10. Time variation of TIBL height for different cases in pre-monsoon 2003 and SW Monsoon 2002

Turbulence Kinetic Energy (TKE) is a measure of the intensity of turbulence in the ABL. TKE at different levels are estimated from the variance of the horizontal and vertical velocity components of Mini-Sodar. The diurnal variation of TKE at different heights is shown in Figs. 9(a&b) in pre-monsoon (28 April 2003), SW monsoon (13, 14 August 2002). The time variation of TKE at different heights follows a wave like pattern which indicates the effect of various scales (meso/large) in the ABL. The TKE is found to increase during the sea breeze onset and in transition hours. A minimum of TKE is observed during other times. TKE estimated from Mini-Sodar shows an increase with height upto 200 m in summer and SW monsoon. A high value of  $\sigma_\theta$  associated with weak wind is noticed in the morning transition hours, 0500-0600 hr (IST) [Fig. 9(a) and Fig. 4(a)] in summer on 28 April. During the SW monsoon, the maximum TKE occurred at 1100 (IST) on 13 August and at 1500 hr (IST) on 14 August, again coinciding with a high value of  $\sigma_\theta$  [Fig. 9(b)].

The maximum TKE during sea breeze and transition periods varies in different seasons. During SW monsoon the maximum TKE is about 8 and 12  $\text{m}^2 \text{s}^{-3}$  during the onset of sea breeze [Fig. 9(b)]. In summer, on 28 April, the maximum TKE during sea breeze hours is  $\sim 6\text{-}8 \text{ m}^2 \text{s}^{-3}$  and during transition time,  $9.6 \text{ m}^2 \text{s}^{-3}$  at 190 m. During the day the mean TKE is  $\sim 3 \text{ m}^2 \text{s}^{-3}$  during SW monsoon and  $3\text{-}4 \text{ m}^2 \text{s}^{-3}$  during summer. This shows the combined effect of local meso-scale circulations and large scale flow on TKE during the monsoon and summer. However, this diurnal variation of TKE in different seasons has to be

studied further with more intensive measurements using fast response instruments such as sonic anemometer.

### 3.3. Mini-Sodar derived TIBL height

Air passing over different surfaces (*viz.*, sea to land) must adjust to the ambient boundary conditions at the new surface. The air which is modified by the new surface properties is said to be confined to an internal boundary layer within the ABL. At land-sea interface, due to day time heating strong gradient of temperature/heat flux develops, leading to formation of a thermal internal boundary layer by sea breeze inflow (Garratt, 1990). Thermal Internal Boundary Layer (TIBL) develops during day time as the cool air over the sea passes over the warm land and produces changes in surface heat fluxes. The height of TIBL can be estimated from the potential temperature profile as well as profile of sensible heat flux.

The temperature flux (sensible heat) has been calculated from sodar data following the method proposed by Weill *et al.* (1980). This method relies on the following relationship between  $\sigma_w$  and the production terms of turbulence, derived from similarity theory (Venkatesan *et al.* 1995)

$$\sigma_w^2 = A [z (\varepsilon_1 + \delta\varepsilon_2)] \quad (1)$$

where  $\varepsilon_1 = u' w' (\partial u / \partial z)$ ,  $\varepsilon_2 = w' \theta'_v (g/\theta_v)$ , 'A' and  $\delta$  are universal constants and  $\theta_v$  is virtual potential temperature. In a dry convective layer ( $\theta_v \cong \theta$ ) when the convective processes dominate (Fiacconi *et al.*, 1997) we can assume that the mechanical production of turbulence is negligible and Eqn. (1) can be further simplified to

$$\frac{\sigma_w^3}{z} = \delta^{\frac{3}{2}} \frac{g}{\theta} w' \theta' \quad (2)$$

$$[\delta = 1.4]$$

From this relation, it results that the value of the ratio  $\sigma_w^3 / z$  is directly proportional to the heat flux at the same height  $z$ , and hence it is possible by means of a Doppler sodar to reconstruct the vertical profile of the ratio and then evaluate the flux. Eqn. (2) is valid in the lower part of the mixed layer especially for a shallow convective layer.

The variation of  $\sigma_w^3 / z$  is similar to the change of  $\sigma_w^2$  and depends on the buoyancy and mechanical turbulence which occur intensively at the surface and generally more in neutral and unstable layer than those in stable layer.



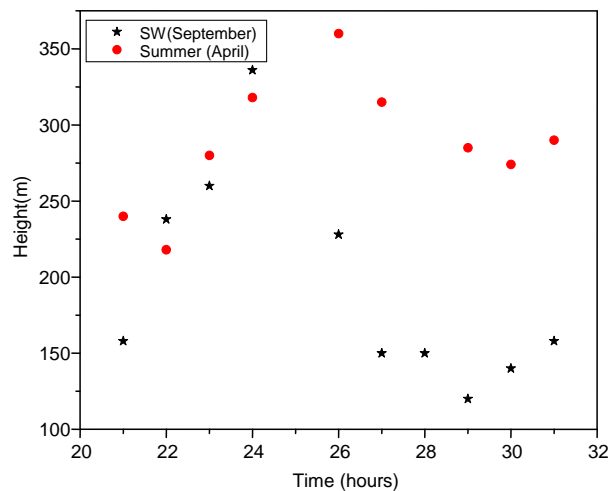


**Fig. 11.** Time variation of NBL height for different cases in pre-monsoon 2003 and SW Monsoon 2002

The TIBL height determined from vertical velocity variance profile varies in different seasons as shown in Fig. 10. 140-170 m in pre-monsoon, 150-225 m in SW monsoon. Seasonal variation in TIBL height can be attributed to the variation in the land - sea temperature difference, strength of the synoptic wind and its direction during different seasons.

#### 3.4. Nocturnal Boundary Layer (NBL) height

The Nocturnal Boundary Layer height for different seasons has been determined using mean wind profile. To determine the NBL height, various depth scales are proposed by different authors: the height at which the turbulence level drops to a small fraction of the surface level (Stull, 1988, Singal, 1989, Kaimal and Finnigan 1994), the height of the peak of the velocity profile (Kaimal and Finnigan, 1994) and so on. From the mean wind profile during the night, the peak velocity (low level wind maxima) has been taken as the NBL height (Murthy *et al.*, 1996) in this study. It is clearly seen in Fig. 11 that the NBL height varies with time in different seasons. The average height of NBL during SW monsoon (3 - 7 and 11 - 14 September 2002) reaches its peak value of 340 m at 2400 hr (IST) and decreases to 125 m at 0500 hr (IST). The NBL height during pre-monsoon (26 - 30 April 2003) was around 375 m at 0200 (IST).

## 4. Conclusion

Analysis of Mini-Sodar measurements during SW monsoon 2002 and pre monsoon season 2003 of the wind and turbulence structure and the development of

ABL/TIBL and NBL on the east coast at Kalpakkam reveals the following :

(i) Significant variations occur in the mixed layer height, ABL winds, vertical velocity variance and TKE during SW monsoon seasons.

(ii) Sudden changes in wind direction at 200-300 m AGL during the onset of sea breeze which was more significant in SW monsoon.

(iii) Large standard deviations in vertical velocity variance were observed during the onset of sea breeze during different seasons.

(iv) The thermal internal boundary layer varies in height during different seasons: 170 m in pre monsoon season 2003, and 210 m in SW monsoon 2002. The corresponding NBL height was about 375 and 340 during pre-monsoon and SW monsoon season respectively.

#### Acknowledgements

The authors sincerely thank Dr. Baldev Raj, Director, Dr. Govindarajan, AD, Safety Group and Dr. A. Natarajan, former Head, RSD, IGCAR, Kalpakkam, for the support and consent given to present and publish this work. Thanks are also due to Scientists at IITM, Pune for their valuable comments and suggestions.

#### References

- Bagavathsingh, A., Somayaji, K. M., Venkatesan, R., Srinivas, C. V., Prakash, G. S., 2003, "A portable acoustic sounding system (Mini-Sodar) for wind and turbulence measurements: Report on installation and recommendation of a suitable operational mode", *Research Report*, No. IGC-256.
- Cresenti, G. H., 1997, "A look back on two decades of Doppler Sodar comparison studies", *Bulletin of American Meteorological Society*, **78**, 4, 651-673.
- Fiacconi, S., Pedesini, M. I., Cassardo, C. and Frustaci, G., 1997, "Validation of a method for the determination of sensible heat flux with sodar data in free convection conditions", *Nuova Cimento (Society for Physics, Italy)*, Vol. **20 C**, No 4.
- Garratt, J. R., 1990, "The internal boundary layer - A Review", *Boundary Layer Meteorology*, **50**, 171-203.

- Kaimal, J. C. and Finnigan, J. J., 1994, "Atmospheric boundary layer flows: Its structure and measurement", Oxford University Press, New York, p289.
- Lenchow, H., 1986, "Probing the Atmospheric boundary layer", *American Meteorological Society, Boston, MA*, p269.
- Murthy, B. S., Dharmaraj, T. and Vernekar, K. G., 1996, "Sodar observations of the nocturnal boundary layer at Kharagpur India", *Boundary Layer Meteorology*, **81**, 201-209.
- Scientec. , 2001, "Minisodar Manufacturers brochure".
- Singal, S. P., 1989, "Acoustic sounding stability studies encyclopedia on environment technology", Vol. 2, Tata McGraw-hill publisher.
- Stull, R. B., 1988, "Introduction to boundary layer meteorology", Kluwer Academic Publishers, The Netherlands, p680.
- Somayaji, K. M., 1991, "Atmospheric studies with sodar at Kalpakkam", *Research Report*, No. IGC-125.
- Thara Prabha, V., Venkatesan, R. and Somayaji, K. M., 1999, "Coastal atmospheric boundary layer experiment (CABLE-98)", Report on the estimation of Site specific parameters, *Research Report*, No : IGC-213.
- Thara Prabha, V., Venkatesan, R., Erich Mursch-Radlgruber, 2002, "Thermal internal boundary layer characteristics at a tropical coastal site as observed by a Mini-Sodar under varying synoptic conditions", *Indian Acad. Sci. (Earth Planet. Sci.)*, **111**, 1, 63-77.
- Venkatesan, R., Sitaraman, V. and Manju. M., 1995, "Estimation of the atmospheric surface layer parameter and comparison with sodar observations", *Atmospheric Environment*, **29**, 22, 3325-3331.
- Weill. A., Klapisz, C., Stauss, D., Bandin, F., Jaupart, C., Van Grudeerbeeck, P. and Goutorbe, J. P., 1980, "Measuring heat flux and structure functions of temperature fluctuations with an acoustic Doppler sodar", *J. Appl. Meteorol.*, **19**, 199-205.
-